Available online at www.sciencedirect.com
ScienceDirect
Journal of Solid State Chemistry 180 (2007) 2790–2797
JOURNAL OF SOLID STATE CHEMISTRY
www.elsevier.com/locate/jssc

Hydrated surface structure and its impacts on the stabilization of t-ZrO_2

Hui Wang[a], Guangshe Li[a], Yanfeng Xue[b], Liping Li[a,*]

[a]*State Key Laboratory of Structural Chemistry, Fujian Institute of Research on the Structure of Matter, Graduate School of Chinese Academy of Sciences, Fuzhou 350002, PR China*
[b]*Department of Physics, Jilin University, Changchun 130023, PR China*

Received 22 May 2007; received in revised form 26 July 2007; accepted 10 August 2007
Available online 29 August 2007

Abstract

We first optimized the preparation conditions to 3.6–6.0 nm ZrO_2 in a pure tetragonal structure (t-phase). All samples were characterized by X-ray diffraction, high-resolution transmission electron microscope, thermal analysis, Raman spectra, and infrared spectra. It is found that the surfaces of t-ZrO_2 nanostructures were terminated by an amorphous hydration layer co-existing with small amounts of carbonate molecules. With the removal of hydrated surface layers under hydrothermal conditions at $T>150\,^{\circ}C$, t-ZrO_2 nanostructures became thermodynamically unstable, which partially transformed into monoclinic ZrO_2 (m-phase). Such a transformation occurs initially at surface regions and then develops into the bulk. High-temperature annealing in air could also remove the hydrated surface layers, which is however followed by a gradual transformation of t-ZrO_2 into m-ZrO_2 in both bulk and surface regions. These observations are explained in terms of the difference in surface free energies of m-ZrO_2 and t-ZrO_2 upon H_2O adsorption.

Keywords: Tetragonal ZrO_2; Hydrothermal process; Hydrated surface structure

1. Introduction

ZrO_2 exhibits three primary polymorphs that are stabilized at different temperature ranges: monoclinic (room temperature—1175 °C), tetragonal (1175–2370 °C), and cubic (2370–2680 °C) [1]. Among these polymorphs, tetragonal phase has received considerable attention due to its wide applications in a number of technologies, including fuel cell electrolytes, catalysts, oxygen sensor, damage-resistant optical coatings, and gate dielectric [2–4]. Tetragonal ZrO_2 is thermodynamically metastable at ambient conditions and is thus unfavorable for applications. Scientific activities have been devoted to stabilize tetragonal ZrO_2 [5]. It is reported that high-temperature tetragonal phase can be stabilized to room temperature provided ZrO_2 particles show a dimension less than a critical size [6]. Various chemical methods [7–10] including sol–gel and precipitation, have been extensively studied to prepare small sizes of ZrO_2. A precise phase control and chemical uniformity of pure t-phase of ZrO_2 are still very difficult to achieve.

Hydrothermal synthesis has been proved to be advantageous in homogenous nucleation for size processing and property tailoring. For example, high-temperature (above 180 °C) hydrolysis of aqueous solution of zirconium salts including zirconyl nitrates and zirconium oxyacetate leads to the formation of almost pure monoclinic structure under hydrothermal conditions [11,12]. While when zirconium hydroxide was used as precursor and treated by a similar hydrothermal condition, the product composed of predominately tetragonal phase and minor monoclinic phase [12]. There are two strategies that are frequently used to obtain phase-pure t-ZrO_2: one is adding some organic additives like polyhydric alcohols and tri-ethanolamine [13,14], another one is adopting appropriate mineralizers [15–17]. However, using these strategies, certain ionic species could be strongly chemically bonded to the sample surfaces, as a result, the roles that these additives have played in the crystallization of zirconia are poorly understood, which limits the systematic study of stabilization and further applications of pure t-ZrO_2.

*Corresponding author. Fax: +86 591 83714946.
E-mail address: lipingli@fjirsm.ac.cn (L. Li).

0022-4596/$ - see front matter © 2007 Elsevier Inc. All rights reserved.
doi:10.1016/j.jssc.2007.08.015

In this work, we optimized the preparation conditions to pure phase t-ZrO_2. All particle sizes were controlled in the range of 3.6–6.0 nm. We found that the surfaces of all t-ZrO_2 nanoparticles were terminated with hydration layers. With removal of the surface hydration layers, all t-ZrO_2 nanoparticles became thermodynamically unstable and partially transformed into a monoclinic phase.

2. Experimental section

Pure tetragonal ZrO_2 nanocrystals were prepared by hydrothermal conditions. Firstly, zirconium hydroxide precursor was prepared by adding 50 mL of 0.5 mol/L $ZrOCl_2 \cdot 8H_2O$ solution to ammonia solution (5 wt%) to reach pH = 10.5. The obtained white precipitate was filtered and sufficiently washed with deionized water till no chlorine could be detected. This precipitate along with 25 mL of 4 M NaOH solution (for certain parallel runs, KOH and ammonia solutions with given concentrations were also used) was transferred to Teflon-lined autoclaves which were allowed to react at varied temperatures from 90 to 220 °C in an oven for 3 h. The products were collected after washing with distilled water until pH = 7, and dried at 60 °C for 3 h. The final samples thus obtained were named as Z90, Z100, Z110, and so on, in which the numbers denote the reaction temperatures. The NaOH concentration was also varied from 0.5 to 16 M to study the influence of mineralizer concentration on the formation of tetragonal ZrO_2. To investigate the structural stabilities of pure tetragonal ZrO_2 nanocrystals, sample Z100 was divided into several parts, which were annealed at 400, 500, 600, and 700 °C in air for 2 h, respectively.

The chlorine contents of our samples were examined using precipitation method, in which parts of the as-prepared samples were dissolved in the concentrated HNO_3 solution under ultrasonication and then reacted with 3 M $AgNO_3$ solution. No turbid precipitates were observed, indicating the absence of chlorine in our samples. X-ray diffraction (XRD) patterns of the samples were recorded on Rigaku D/MAX 2500 diffractometer with Cu$K\alpha$ radiation. Nickel powders with a purity of 99.9% were used as the internal standard for peak position determination. The crystalline sizes were calculated from the peak broadening of the most intense XRD peak (101) for tetragonal phase and $(\bar{1}\,1\,1)$ for monoclinic phase according to Scherrer formula, $D = 0.9\lambda/\beta \cos\theta$, where λ is the X-ray wavelength used and β is the half-width. The particle shape and size were examined by high-resolution transmission electron microscope (HRTEM) image, and the chemical compositions were determined by energy-dispersive X-ray analysis (EDXA). Thermal behaviors of the samples were investigated using STA449C Jupiter-QMS 403C Aëolos at a heating rate of 15 °C/min. Fourier transform infrared spectra of the samples were measured on Perkin-Elmer Spectrum One FTIR Spectometer at a resolution of 4 cm^{-1} using KBr pellet technique. Raman spectra of the samples were recorded using a JY-HR800 spectrometer with a He–Ne laser. The excitation wavelength is 632.8 nm and output powder is 20 mW.

3. Results and discussion

3.1. Optimized preparation conditions to t-ZrO_2

NH_4OH, KOH, LiOH, and NaOH could act as the mineralizers for stabilization of tetragonal ZrO_2. When using NH_4OH as the mineralizer, the product was amorphous after hydrothermal reactions at 130 °C for 2 h. When using KOH, similar reaction conditions gave rise to a mixture of tetragonal and monoclinic phases. Comparatively, LiOH has already been reported not suitable for stabilization of tetragonal ZrO_2 [17]. In this work, we explored the preparation of tetragonal ZrO_2 using NaOH as the mineralizer.

Firstly, we studied the phase evolution of t-ZrO_2 as a function of NaOH concentrations at a fixed reaction temperature of 110 °C. As indicated in Fig. 1, when NaOH concentration is 0.5 M, the product was a mixture of tetragonal and monoclinic phases. When the NaOH concentration is higher than 1 M, the product is tetragonal ZrO_2, showing XRD profiles matching well the standard diffraction data of tetragonal ZrO_2 (JCPDS No. 42-1164). Further increasing NaOH concentration did not give any extra diffraction peaks but the broadened diffraction peaks, which indicated the formation of small particle sizes of tetragonal ZrO_2.

Secondly, we studied the phase evolution of ZrO_2 as a function of reaction temperature at a fixed NaOH concentration of 4 M. As indicated in Fig. 2, when the reaction temperature is 90 °C, the products are amorphous as characterized by several dispersed peaks. When the reaction temperature was increased beyond 100 °C, tetragonal ZrO_2 was formed with its diffraction intensity being increased with the reaction temperature. The stabilization of tetragonal ZrO_2 was also confirmed by

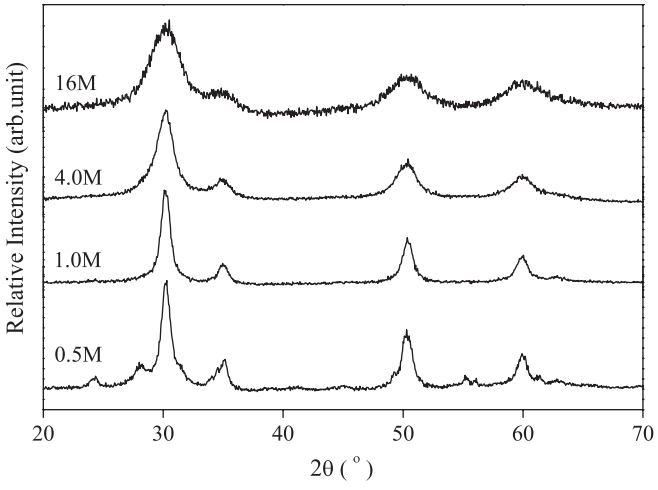

Fig. 1. XRD patterns of the samples obtained at 110 °C using different NaOH concentrations.

TEM observations (Fig. 3), in which highly crystalline ZrO_2 was seen in spite of an obvious agglomeration. Average particle size of the samples obtained at 110 °C was 4 nm, which is compatible with that of 4.8 nm calculated by XRD peak broadening. The interplanar spacing for (101) plane measured by HRTEM (Fig. 3b) is almost the same as that obtained for tetragonal ZrO_2 by XRD structural refinements. Compositional analysis for all single-phase samples by EDXA indicated the presence of Zr only. These results showed that our tetragonal ZrO_2 nanocrystals are chemically pure at ambient conditions. Tetragonal phase was stable below 130 °C, which transformed into monoclinic phase with further increasing the reaction temperature higher than 150 °C. This phase transformation is also accompanied by changes in particle sizes. The qualitative phase analysis and particle sizes are presented in Table 1. It is seen that the grain size of *t*-ZrO_2 increased from 3.6 to 7.2 nm when temperature varied from 100 to 150 °C and then decreased with increasing temperature. Correspondingly, the grain size of *m*-ZrO_2 increased from 7.2 to 20.6 nm when temperature was elevated from 150 to 200 °C and then varied little with further increasing temperature. These observations demonstrated that the critical size for tetragonal-monoclinic transition is about 7 nm under the present hydrothermal conditions.

Therefore, mineralizers and reaction temperature play the critical role in the phase composition and particle sizes of ZrO_2. This could be understood by taking into account the crystallization processes of zirconia. The crystallization of ZrO_2 nanocrystals mainly consists of nucleation and grain growth processes. When $ZrOCl_2 \cdot 8H_2O$ was dissolved into an aqueous solution, tetramer complexes, $[Zr_4(OH)_8(H_2O)_{16}]^{8+}$, would form as a major species. The tetramer has 8 hydroxo bridges and 16 coordinate

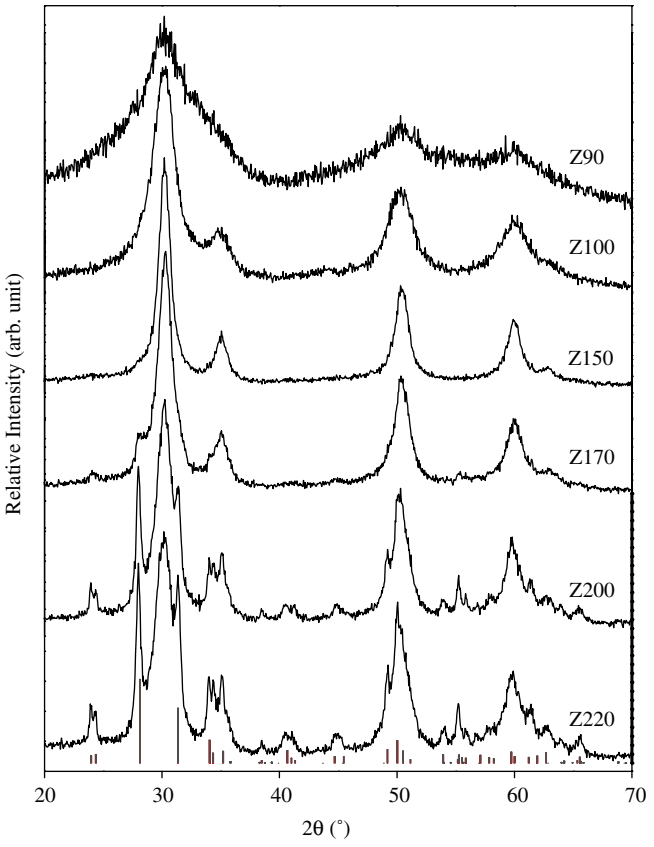

Fig. 2. XRD patterns of the samples obtained at given temperatures using a fixed NaOH concentration of 4 M. Vertical bars below the patterns represent the standard diffraction data from JCPDS file for monoclinic ZrO_2 (No. 37-1484).

Table 1
Phase compositions and particle sizes of the samples synthesized at different reaction temperatures at the presence of 4 M NaOH

Samples	Tetragonal ZrO_2		Monoclinic ZrO_2	
	Content (%)	Size (nm)	Content (%)	Size (nm)
Z100	100	3.6	0	–
Z110	100	4.9	0	–
Z130	100	6.0	0	–
Z150	91	7.2	9	7.2
Z170	85	5.9	15	12.2
Z200	69	5.7	31	20.6
Z220	65	5.2	35	19.3

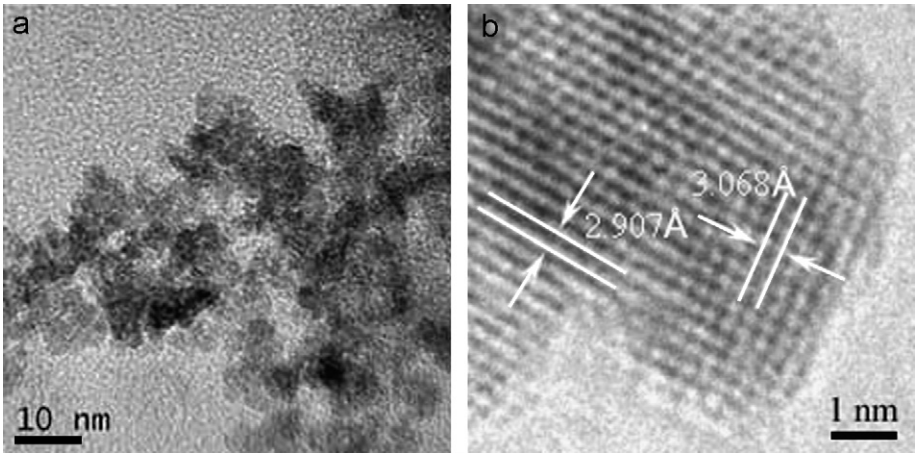

Fig. 3. TEM photo (a) and HRTEM images (b) of Z110.

water molecules [18]. When this solution was heated or dropped into strong basic solution, tetramer would release certain amounts of H^+ ions from the coordinated water in terms of the following equation:

$$[Zr_4(OH)_8(H_2O)_{16}]^{8+} \rightarrow [Zr_4(OH)_{8+x}(H_2O)_{16-x}]^{(8-x)+} + xH^+.$$

Polymerization might proceed by olation among $[Zr_4(OH)_{8+x}(H_2O)_{16-x}]^{(8-x)+}$. When the concentration of polymeric species reaches a critical level, ZrO_2 nuclei would occur [19]. This procedure depends on the mineralizers used. For the solution containing neutral mineralizers, such as NaCl and KBr, high temperature was usually necessary to promote the polymerization [15]. However, high temperature is not beneficial for the stabilization of t-ZrO_2 since tetragonal phase is thermodynamically metastable. As stated above, NaOH when involving in the hydrothermal processes can lead to the formation of crystalline ZrO_2 at 100 °C, therefore it is probable that hydrolysis and condensation of tetramers were promoted by high concentration of OH^- in the solution.

Apart from anions (OH^-), alkali ions from the mineralizers MOH ($M = Na^+$, K^+, and NH_4^+) also affect the crystallization process of ZrO_2. A previous investigation [17] has shown that increasing radius size of cationic would cause the decrease of crystalline rate of ZrO_2. In our experiments, we found that a mixture of m- and t-ZrO_2 was formed when 4 M KOH was employed as the mineralizer. Compared with K^+, Na^+ favors the formation of tetragonal structure. Chen et al. [20] studied the effect of Na^+ on thermal behavior of hydrous ZrO_2 and also found that Na^+ can promote the formation of t-ZrO_2 while preventing the transformation from tetragonal to monoclinic phase. They concluded that Na^+ species might incorporate into the surface vacant sites and thus stabilize t-ZrO_2. From the chemical compositions of our samples experimentally measured by EDX analysis and precipitation method, we may conclude that all these adsorbed Na^+ species are loosely bonded to the surfaces of as-prepared ZrO_2 nanoparticles and therefore can be removed after sufficient washings, although these Na^+ species have already played significant impacts on the crystallization of t-ZrO_2. Furthermore, reaction temperature seems to have certain impacts on the tetragonal stabilization since when reaction temperature is increased up to 160 °C or higher, phase transformation from tetragonal to monoclinic occurred, regardless of the Na^+ concentration.

3.2. Surface hydration structure of t-ZrO_2 nanocrystals

Raman spectroscopy is a surface-sensitive technique. Here, we used Raman spectra to monitor the surface structure of ZrO_2 nanoparticles. Fig. 4 shows Raman spectra of the samples obtained at different temperatures. When the reaction temperature is intermediate between 90 and 130 °C, three broad peaks were observed in the Raman shift region from 100 to 900 cm^{-1}, which are associated with long-range disordering arrangement in amorphous state. These observations seemed not consistent with our XRD data and TEM images since for the latter cases, ZrO_2 nanoparticles were seen to show a rather good crystallinity at the absence of amorphous phases (Figs. 2 and 3). Therefore, it is most likely that there exists a hydrated amorphous layer at the surface of tetragonal ZrO_2.

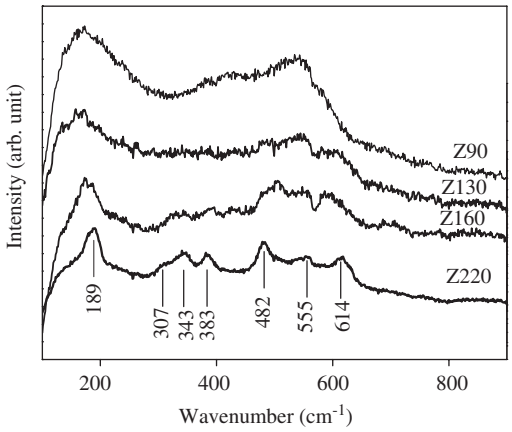

Fig. 4. Raman spectra for typical samples obtained at different temperatures.

This hydrated amorphous layer was also indicated by the broad Raman peaks when the reaction temperature was increased up to 160 °C. When the reaction temperature is beyond 160 °C, several weak Raman peaks appeared at about 185, 345, and 383 cm^{-1}, which are assigned to the intrinsic vibration modes of monoclinic ZrO_2 [21,22]. When the reaction temperature was further increased up to 220 °C, broad Raman peaks associated with the hydrated amorphous layers were completely gone except for the strong Raman peaks for monoclinic ZrO_2. It is noted that the Raman spectra of these samples did not indicate the presence of any traces of tetragonal ZrO_2, which seems not consistent with our XRD analysis (Table 1), since for the latter case, the composition of tetragonal component is calculated to be at least 65% when the reaction temperature is increased up to 220 °C. Therefore, it is likely that the samples prepared in the temperature range from 160 to 220 °C may have a sandwich structure, in which the monoclinic phase existed in the intermediate layers between the inner tetragonal ZrO_2 core and the top amorphous hydrated layers. The transformation of ZrO_2 from tetragonal to monoclinic structure might take place initially at surface regions and then develop into the bulk with increasing the reaction temperatures, which is consistent with the results reported by Li et al. [23].

Surface hydration structure of t-ZrO_2 nanocrystals was also investigated by IR spectrum. Fig. 5 shows the IR spectrum of a typical sample Z100. There are a strong broad absorption centered around 3413 cm^{-1}, three sharp absorption bands at about 1630, 1352, and 960 cm^{-1}, and

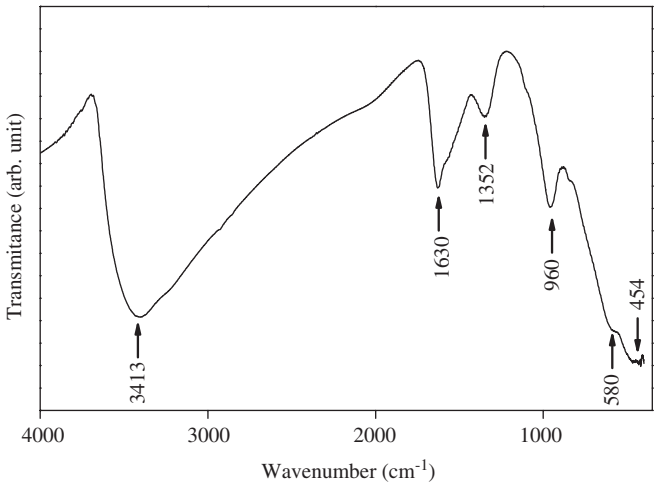

Fig. 5. IR spectrum for Z100.

two weak absorption bands at 580 and 454 cm^{-1}. The bands at about 580 and 455 cm^{-1} correspond to E_u mode of Zr–O vibration of tetragonal structure [24]. The absorption band located around 3413 cm^{-1} is associated with the O–H stretching vibration of adsorbed water and hydroxyl group, while the absorption band at 1630 cm^{-1} is due to the bending mode of associated water [25]. The observation of a strong broad absorption at 3400 and sharp absorption band at 960 cm^{-1} implied that the hydration molecules could be in several different energetically bonding states. The hydrated amorphous terminations are highly reactive in forming carbonate species on the surfaces by adsorbing atmospheric CO_2 [26], as indicated by the presence of absorption band at 1352 cm^{-1}. Mass spectra of the exhaust gases of the as-prepared samples during heating processes confirmed the presence of CO_3^{2-} species absorbed on surfaces of t-ZrO_2 nanocrystals, which will be described latter.

Thermal behaviors associated with the surface hydration of t-ZrO_2 nanocrystals were examined by thermogravimetric analysis (TGA) technique. All t-ZrO_2 nanocrystals showed a similar mass loss in a wide temperature range from room temperature to 900 °C (Fig. 6a). These surface hydration terminations were completely removed when the temperatures is higher than 900 °C, as is indicated by the almost constant mass. The total amount of mass loss for hydration removal was determined to be 13.5 wt% for sample Z100, while the surface terminations for Z220 became less, as indicated by a significant decrease of mass loss at 6.7 wt%.

The exhaust gases released during the heating process were examined by mass spectroscopy (MS). Fig. 6b shows the MS signals for sample Z100. In the temperature range from room temperature to 1000 °C, only water and CO_2, corresponding to the $m/Z = 18$ and 44, respectively, were detected. It should be emphasized that the ionic current for CO_2 signal is only about 25th of that for H_2O signal, which implied that the amount of CO_2 is qualitatively very low in the exhaust gas in comparison with water. Therefore, the total mass loss observed at temperatures up 600 °C should

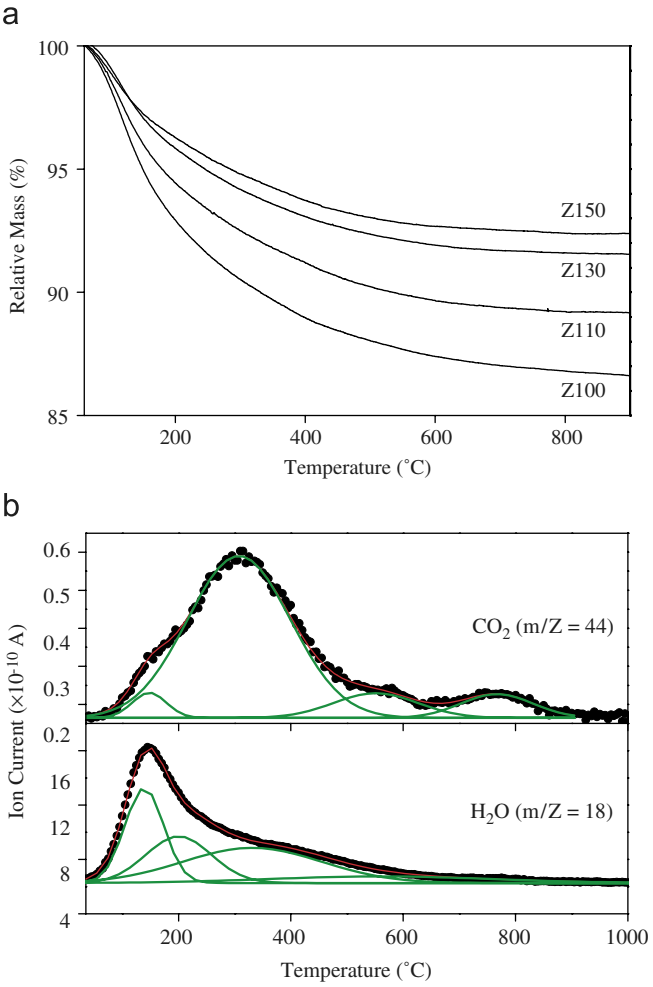

Fig. 6. TGA curves (a) of t-ZrO_2 and MS curves (b) of Z100.

be contributed mainly from surface hydration termination. Careful analysis of MS signals can help us to determine the bonding states of H_2O and CO_2 with the surfaces of t-ZrO_2 nanocrystals. As shown in Fig. 6b, a broad and relatively strong peak between 30 and 650 °C as well as a weak peak above 650 °C were observed for CO_2 signal. The MS signal of CO_2 could be evidently deconvoluted into four Gaussian curves centered at 150, 310, 560, and 760 °C, which indicated at least four kinds of energetically nonequivalent group that surface carbonate molecules are coordinated with nanocrystals. Similarly, H_2O signal can also be deconvoluted into four components with peak positions at 140, 200, 330, and 530 °C, respectively. The first one with low-temperature peak at 140 °C is attributed to physisorbed water, while the components with temperature peak at 200 and 330 °C are from chemisorbed water [27]. The last one centered at 530 °C is very weak, which is associated with the low concentration of residual surface hydroxyls at high temperatures. This reasoning is consistent with the general observation that most of the surface hydration layers of almost the other oxide nanoparticles, just like TiO_2, Fe_2O_3, and MgO, have already been removed at temperatures below 530 °C [28–30]. Basing on the desorbed

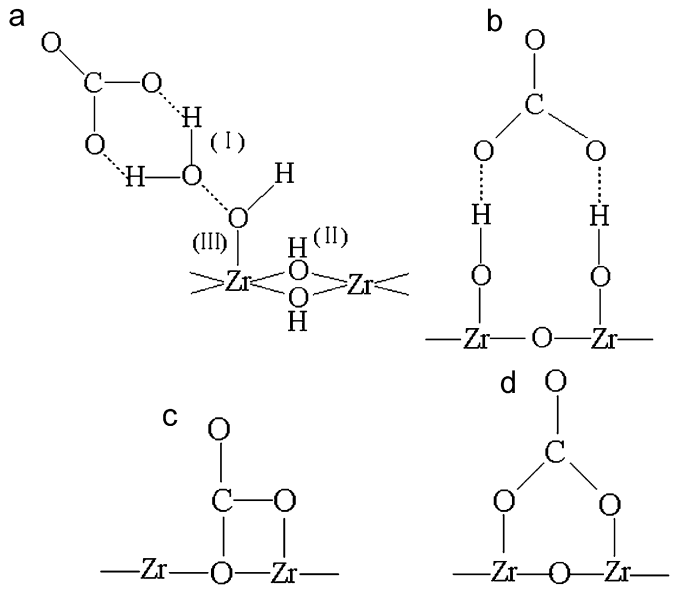

Fig. 7. Structure model proposed for the surface hydration and carbonates of t-ZrO_2.

temperatures of H_2O and CO_2, we proposed a coordinated model to describe bonding states of surface hydration and carbonate molecules. In Fig. 7a, configuration I denotes the physisorbed water molecules that would be dehydrated at 140 °C, while both configurations II and III represent the chemisorbed water molecules that would be dehydrated at 200 and 310 °C, respectively. Among these three kinds of surface hydration molecules, configurations I and III are highly reactive to CO_2 to give two kinds of surface carbonate molecules (Figs. 7a and b). The carbonate molecules bounded with physisorbed water (configuration I) would first decompose at 150 °C (Fig. 7a), while those associated to chemisorbed water (Fig. 7b) would be desorbed at 310 °C. The other two kinds of carbonate molecules interacted with the surface lattice oxygen and Zr ions through Figs. 7c and d to form comparatively stable absorptions, which would decompose at as high as 560 and 760 °C, respectively. From Fig. 6b, it is seen that, for sample Z100, the carbonate molecules bonding to the chemisorbed water are the main component (taking about 79.8% of total surface carbonate molecules). On the contrary, the carbonate molecules bonded to physisorbed water is estimated to be only about 3.8%, indicating a very weak bonding state that could be easily desorbed. It is also noted that the proportions of carbonate molecules directly bonded with Zr ions and lattice oxygen anions were almost the same (i.e., 8.3% and 8%, respectively), which should be related to the similar amounts of the Zr and oxygen ions exposed on surfaces of t-ZrO_2 nanocrystals.

3.3. Surface hydration structure evolution and stabilization of t-ZrO_2

Surface structure evolution of t-ZrO_2 during heating processes was investigated by XRD in combination with

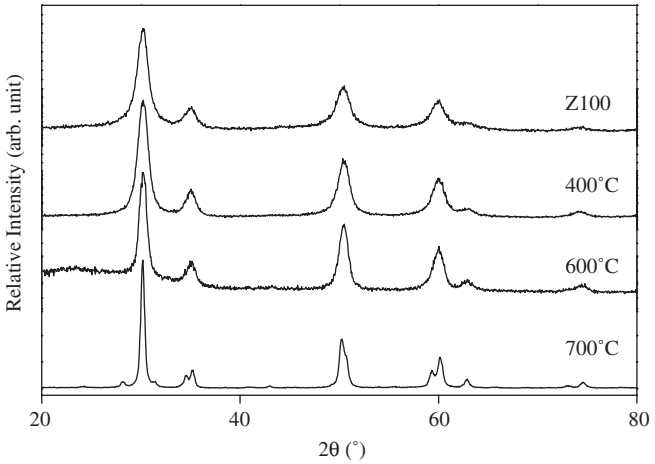

Fig. 8. XRD patterns of the ZrO_2 samples obtained after sintering at different temperatures.

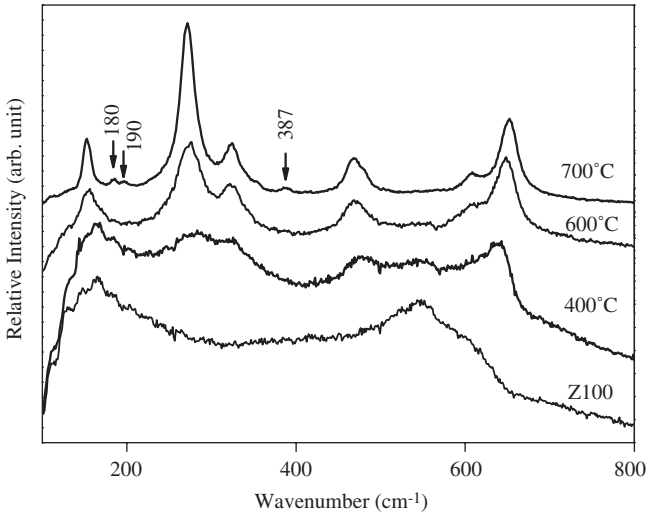

Fig. 9. Raman spectra of the ZrO_2 samples after sintering at different temperatures.

Raman spectrum. Fig. 8 shows the XRD patterns of the samples obtained after heating Z100 at 400, 600, and 700 °C in air for 2 h, respectively. It is seen that tetragonal structure could be stabilized up to 700 °C, which is followed by a grain growth such as from 6.6 to 19.6 nm. While when the treatment temperature is above 700 °C, t-ZrO_2 nanocrystals were partially transformed into monoclinic phase as indicated by the weak diffraction peaks at 28°.

Fig. 9 shows the Raman spectra of the samples after heat treatments. Besides the two broad peaks at 160 and 547 cm^{-1} for Z100, the sample obtained after heating at 400 °C exhibited several weak peaks at 278, 325, 474, and 638 cm^{-1} that are responsible for t-ZrO_2 [31]. The existence of Raman peaks at 160 and 547 cm^{-1} indicates the presence of hydrated amorphous zirconia on surfaces. Further increasing the temperature to 600 °C, the Raman peaks for amorphous structure disappeared and all Raman peaks

are assigned to the t-ZrO_2. The variation of Raman spectra during the heating process is consistent with the dehydration process as revealed by TGA and MS measurement, in which the dehydration almost finished at 600 °C. However, when the temperature was increased to 700 °C, three weak Raman peaks at 180, 190, and 387 cm^{-1} characteristic of m-ZrO_2 are observed in addition to characteristic Raman peaks for t-ZrO_2, which indicated that a small part of t-ZrO_2 has transformed into m-ZrO_2 [32], consistent with our XRD analysis stated above.

Based on these observations, we conclude that surface hydration structure is a key factor that is responsible for the stabilization of t-ZrO_2 nanocrystals. There are two primary ways to alter the surface hydration structure: one is via a direct hydrothermal reaction and another is via a high-temperature treatment, though their impacts on the phase evolution could be significantly different. For example, with increasing hydrothermal reaction temperature, the transformation of ZrO_2 from tetragonal to monoclinic structure could prefer to occur at surface regions, while high-temperature annealing might lead to the homogeneous formation of monoclinic structure in bulk and surface of t-ZrO_2. These distinct phase evolutions are attributed to a decrease in the difference between the surface free energy of m-ZrO_2 and t-ZrO_2 upon surface adsorption of H_2O, since the stabilization temperature range and critical size of t-ZrO_2 in hydrothermal condition were both lower than those of the samples after high-temperature annealing. Therefore, the tetragonal-to-monoclinic phase transformation occurs more easily in solutions. Similarly, Bell et al. [33] also found that t-ZrO_2 transforms into m-ZrO_2 when immersed in water.

4. Conclusions

Tetragonal ZrO_2 nanostructure was prepared by hydrothermal conditions. The effects of temperature and mineralizers on the crystallization and phase composition of ZrO_2 were studied. It is found that high NaOH concentration and appropriate temperature (100–130 °C) facilitate the formation of t-ZrO_2 while low NaOH concentration and higher temperature produce the mixtures of t- and m-ZrO_2. When NaOH was used as mineralizer, the crystallization temperature of ZrO_2 was lowered greatly, which is advantageous for the stabilization of metastable t-ZrO_2. There exists an amorphous hydration layer at the surfaces of t-ZrO_2, which transforms completely into m-ZrO_2 when hydrothermal temperature was increased to 220 °C. By contrast, high-temperature annealing below 700 °C in air led to the transformation of the amorphous structure into t-ZrO_2. When the annealing temperature was further increased up to 700 °C, tetragonal structure partially transformed into monoclinic structure in both bulk and surface regions. The phase stabilization and transformation of t-ZrO_2 demonstrated in this work are fundamentally important, which allows in-depth understanding of the stabilization nature of tetragonal ZrO_2 nanostructures for technological applications.

Acknowledgments

This work was financially supported by NSFC under the contract (No. 20671092), a grant from Hundreds Youth Talents Program of CAS (Li GS), National Basic Research Program of China (2007CB613306) and in part by a Science and Technology Program from Fujian Province (No. 2005HZ01-1, Z0513026).

References

[1] S. Shukla, S. Seal, J. Phys. Chem. B 108 (2004) 3395–3399.
[2] N.N. Zhao, D.C. Pan, W. Nie, X.L. Ji, J. Am. Chem. Soc. 128 (2006) 10118–10124.
[3] D.A. Zyuzin, S.V. Cherepanova, E.M. Moroz, E.B. Burgina, V.A. Sadykov, V.G. Kostrovskii, V.A. Matyshak, J. Solid State Chem. 179 (2006) 2965–2971.
[4] J.L. Gole, S.M. Prokes, J.D. Stout, O.J. Glembocki, R.S. Yang, Adv. Mater. 18 (2006) 664–667.
[5] S. Shukla, S. Seal, Int. Mater. Rev. 50 (2005) 45–64.
[6] R.C. Garvie, J. Phys. Chem. 69 (1965) 1238–1243.
[7] Y.T. Moon, H.K. Park, D.K. Kim, C.H. Kim, I.-S. Seog, J. Am. Ceram. Soc. 78 (1995) 2690–2694.
[8] G. Ehrhart, B. Capoen, O. Robbe, Ph. Boy, S. Turrell, M. Bouazaoui, Thin Solid Films 496 (2006) 227–233.
[9] F.C.M. Woudenberg, W.F.C. Sager, N.G.M. Sibelt, H. Verweij, Adv. Mater. 13 (2001) 514–516.
[10] A.P. Oliveira, M.L. Torem, Powder Technol. 119 (2001) 181–193.
[11] H. Reverón, H. Vesteghem, J. Nanosci. Nanotechnol. 5 (2005) 1643–1650.
[12] Y.V. Kolen'ko, V.D. Maximov, A.A. Burukhin, V.A. Muhanov, B.R. Churagulov, Mater. Sci. Eng. C 23 (2003) 1033–1038.
[13] X.L. Jiao, D.R. Chen, L.H. Xiao, J. Cryst. Growth 258 (2003) 158–162.
[14] D.K. Qin, H.L. Chen, J. Mater. Sci. 41 (2006) 7059–7063.
[15] E. Tani, M. Yoshimura, S. Sōmiya, J. Am. Ceram. Soc. 66 (1983) 11–14.
[16] H.-J. Noh, D.-S. Seo, H. Kim, J.-K. Lee, Mater. Lett. 57 (2003) 2425–2431.
[17] G. Dell'Agli, A. Colantuono, G. Mascolo, Solid State Ionics 123 (1999) 87–94.
[18] G.T. Mamott, P. Barnes, S.E. Tarling, J. Mater. Sci. 26 (1991) 4054–4061.
[19] K. Matsui, M. Ohgai, J. Am. Ceram. Soc. 84 (2001) 2303–2312.
[20] Zh. Liu, W.J. Ji, L. Dong, Y. Chen, J. Solid State Chem. 138 (1998) 41–46.
[21] J.Ch. Valmalette, M. Isa, Chem. Mater. 14 (2002) 5098–5102.
[22] G. Xu, Y.-W. Zhang, Ch.-Sh. Liao, C.-H. Yan, Phys. Chem. Chem. Phys. 6 (2004) 5410–5418.
[23] M. Li, Z. Feng, G. Xiong, P. Ying, Q. Xin, C. Li, J. Phys. Chem. B 105 (2001) 8107–8111.
[24] C. Pecharromán, M. Ocaña, C.J. Serna, J. Appl. Phys. 80 (1996) 3479–3483.
[25] Y.F. Gao, Y. Masuda, H. Ohta, K. Koumoto, Chem. Mater. 16 (2004) 2615–2622.
[26] C.M. Phillippi, K.S. Mazdiyasni, J. Am. Ceram. Soc. 54 (1971) 254–258.
[27] J.-F. Boily, J. Szanyi, A.R. Felmy, Geochim. Cosmochim. Acta 70 (2006) 3613–3624.
[28] G. Li, L. Li, J. Boerio-Goates, B.F. Woodfield, J. Am. Chem. Soc. 127 (2005) 8659–8666.
[29] L. Lu, L. Li, X. Wang, G. Li, J. Phys. Chem. B 109 (2005) 17151–17156.

[30] X.Q. Qiu, G.S. Li, L.P. Li, J. Mater. Res. 22 (2007) 908–912.
[31] G. Xu, Y.-W. Zhang, B. Han, M.-J. Li, C. Li, Ch.-H. Yan, Phys. Chem. Chem. Phys. 5 (2003) 4008–4014.
[32] G. Xu, Y.-W. Zhang, Ch.-Sh. Liao, C.-H. Yan, J. Am. Ceram. Soc. 87 (2004) 2275–2281.
[33] S. Xie, E. Iglesia, A.T. Bell, Chem. Mater. 12 (2000) 2442–2447.